International Journal of Antimicrobial Agents 66 (2025) 107564

Contents lists available at ScienceDirect

International Journal of Antimicrobial Agents

journal homepage: www.elsevier.com/locate/ijantimicag

Large scale laboratory evolution uncovers clinically relevant collateral antibiotic sensitivity

Farhan R. Chowdhury[a], Veronica Banari[b], Vlada Lesnic[b], George G. Zhanel[c], Brandon L. Findlay[a,b,*]

[a] Department of Biology, Concordia University, Montréal, Québec, Canada
[b] Department of Chemistry and Biochemistry, Concordia University, Montréal, Québec, Canada
[c] Department of Medical Microbiology and Infectious Diseases, Max Rady College of Medicine, University of Manitoba, Winnipeg, Manitoba, Canada

ARTICLE INFO

Article history:
Received 8 April 2025
Accepted 26 June 2025

Editor: Prof. Q. Yang

Keywords:
Antibiotic resistance
Collateral sensitivity
Adaptive laboratory evolution

ABSTRACT

The increasing prevalence of antibiotic resistance is a critical challenge, necessitating the development of strategies to mitigate the evolution of resistance. Collateral sensitivity (CS)-based sequential therapies have been proposed to mitigate resistance evolution.

However, the evolutionary repeatability of CS across different experimental conditions and its clinical relevance remain underexplored, hindering its potential for translation into clinical practice. Here, we evolve 20–24 lineages of *E. coli* against tigecycline (TIG) and piperacillin (PIP), antibiotics suggested to produce CS, through three separate laboratory adaptive evolution (ALE) platforms to test for the robustness of CS interactions and the effect of the choice of ALE on CS evolution. We generate over 130 resistant mutants and 540 resistance and collateral sensitivity measurements to identify a CS relationship between TIG and polymyxin B (POL) that is highly repeatable across all the ALEs tested, suggesting that this CS interaction is preserved across different evolution microenvironments. We determine the mechanism of this novel CS by showing that cells resistant to TIG deactivate the Lon protease and overproduce negatively charged exopolysaccharides, which in turn attracts the polycationic POL and renders cells hypersensitive to the drug. We find that this CS relationship is present in a clinical dataset of over 750 uropathogenic MDR *E. coli* isolates, and show that the soft agar gradient evolution (SAGE) platform best predicts collateral effects (CS, neutrality or cross resistance) in this dataset. Our study provides a framework for identifying robust CS with clinical implications that can reduce the emergence of resistance to our existing antibiotics.

1. Introduction

Antibiotic resistance is spreading at an alarming rate, claiming the lives of over 1.2 million people every year [1]. Developing strategies to slow down resistance evolution has become essential to combat antibiotic resistance [2]. Sequential antibiotic therapy, where antibiotics are administered in a chronological sequence in an individual patient, has emerged as a potential strategy to slow down the evolution of resistance [3]. In principle, this strategy interrupts the selection of resistant populations by changing the selective pressure via switching treatment to a different drug [4]. Evolutionary trade-offs like collateral sensitivity (CS) have been proposed to improve the success of such sequential therapies by limiting the rate of bacterial evolution [5–7]. We now have numerous studies that have described large networks of collateral sensitivities in different bacteria [6,8–11]. However, investigations on their evolutionary repeatability via large scale experimental evolution are scarce, but are essential for successful clinical application [12]. In addition, different laboratories use different adaptive laboratory evolution (ALE) platforms that are difficult to standardize [6,8,9,13,14]. Since evolutionary outcomes can vary depending on the bacterial microenvironment [12,15], it is important to determine the effect of the choice of the ALE platform on CS evolution.

In this study, we evolve 20–24 lineages of *Escherichia coli* to screen for CS between four drug pairs reported to exhibit CS, using three different ALE platforms widely used to study evolution and CS [16]. We find that serial transfer and gradient plating-based ALE platforms agree well on the frequencies of CS, cross-resistance (CR) and resistance levels. However, the soft agar gradient evolution (SAGE) platform produces substantially lower frequencies of CS and

* Corresponding author. Mailing address: Department of Biology, Concordia University, Montréal, Québec, Canada.
E-mail address: brandon.findlay@concordia.ca (B.L. Findlay).

https://doi.org/10.1016/j.ijantimicag.2025.107564

higher incidence of CR compared to the other two platforms. To test the relevance of these CS/CR predictions from the different ALE platforms, we analyze antimicrobial susceptibility data from over 750 clinical uropathogenic multidrug resistant (MDR) *E. coli* strains to test for the presence of CS/CR relationships. We find that CS is almost entirely absent, but neutrality or CR is prevalent. However, we observe a significant association between increasing omadacycline (a third generation tetracycline) resistance and reduced colistin (polymyxin E) resistance. Interestingly, out of the four drug pairs screened in our ALE experiments, SAGE showed significant CS in only one of them: a tigecycline (TIG) (a third generation tetracycline) and polymyxin B (POL) pair. Using genomics and phenotypic analysis, we describe, for the first time, the mechanism of polymyxin B CS in tigecycline-resistant bacteria. Our results highlight the power of large-scale ALE experiments in predicting repeatable CS relationships that hold potential to reduce resistance in MDR bacteria in the clinic.

2. Results

2.1. SAGE produces lower collateral sensitivities and higher cross resistances compared to other ALE platforms

We evolved 20–24 mutants against tigecycline (TIG) and piperacillin (PIP) separately using three different ALE platforms [16]: SAGE [17], serial transfer liquid culture-based method (LQ) [18], and gradient plates (GP) [19] (Fig. 1A). We also investigated CS profiles for nitrofurantoin (NIT) and ciprofloxacin (CIP), but were unable to achieve resistance at high enough frequencies in LQ (NIT, CIP) or GP (CIP) to generate the necessary sample sizes (Supplementary Table 1). SAGE also produced 8–16-fold increases in relative MIC (MIC of evolved lineage/MIC of WT) of TIG and PIP, while levels from LQ and GP were limited to 2–4-fold increases (Fig. 1B, C) before incurring frequent extinctions. SAGE presents a smooth continuous gradient of antibiotic in soft agar instead of the 2-fold stepwise increasing gradients present in the serial transfer-based method (LQ) [17]. Because of this, SAGE allows selection of small-effect mutations which may not confer resistances high enough to survive in 2-fold increasing gradients [20]. These mutations may help explain the higher MICs reached through SAGE. Even in GP, daily passaging of a random mutant in the plate introduces a sampling bottleneck which may not select cells with small-effect mutations.

Next, we screened for CS towards POL and gentamicin (GEN) in the TIG-resistant lineages [8] and NIT and streptomycin (STR) in the PIP-resistant lineages [6,8]. A large proportion of TIG-resistant lineages exhibited CS to POL: ∼86% from LQ, ∼96% from GP, and ∼39% from SAGE (Fig. 1D) (Supplementary Fig. 1). We previously reported the presence of reciprocal CS between the POL -TIG pair [21]. CS towards GEN was low in all platforms, with LQ and GP showing CS in ∼26% of lineages and SAGE in only ∼4% (Fig. 1E) (Supplementary Fig. 1). Cross resistance (CR) towards POL was almost entirely absent, and CR to GEN was present at very low frequencies (Fig. 1D, E) (Supplementary Fig. 1).

CS towards NIT was rare in the PIP-resistant lineages, present in only ∼17-25% of the LQ and GP strains and absent in the SAGE strains (Fig. 1F) (Supplementary Fig. 1). In contrast CR was common in the SAGE lineages, with ∼42% less susceptible to NIT (Fig. 1F) (Supplementary Fig. 1). About 50% of the PIP-resistant lineages from LQ and GP, and 21% from SAGE showed CS towards STR (Fig. 1G) (Supplementary Fig. 1). ∼20% of the SAGE mutants showed CR towards STR, but again this CR was rare in the other two platforms. Overall, ∼16% of SAGE mutants showed CS compared to 49% and 47% from LQ and GP respectively (Fig. 1H). Incidence of CR in SAGE mutants was much higher at about 21% than the 4-6% in LQ and GP mutants (Fig. 1H).

2.2. Tigecycline resistance evolves via similar pathways across ALE platforms

To compare the genomic adaptations of lineages evolved through the three different platforms and to identify differences in mutational profiles between strains that evolved CS and strains that did not, we whole genome sequenced 29 lineages adapted to TIG: nine from LQ (six with POL CS and three neutral), seven from GP (six with POL CS and one neutral) and 13 from SAGE (six with POL CS, six neutral, and one with POL CR) (Fig. 2A). The genome profile of the lineage that showed POL CR from SAGE was a complete subset of the mutations appearing in the CS lineages, and was excluded from further analysis suspecting a two-fold random variation in MIC [22]. Lineages acquired ∼1.2 mutations per strain from LQ, ∼1.7 strain from GP, and ∼1.5 mutations per strain from SAGE (Fig. 2A). SAGE generated several mutations unique from the other platforms, presumably because it selects for mutants that have improved growth rates and motility [17,20] which are often seen as compensatory mutations in antibiotic resistant bacteria [23–28]. Strains from all platforms showed mutations in one or more of the following genes involved in TIG resistance: *lon, acrR*, and *marR* (Fig. 2A) (Supplementary Fig. 2A). Deactivation of the Lon protease, often achieved via mutations in its promoter region, spares the MarA, RamA and SoxS activators from degradation, increasing expression of genes that mediate resistance like *acrAB* [29,30]. Mutations in AcrR and MarR more directly relieve repression of the *acrAB* and *marRAB* operons, increasing efflux activity to drive TIG resistance [30]. The primary method by which TIG resistance evolved is therefore through increased expression of efflux pumps, regardless of the evolutionary system.

2.3. Polymyxin collateral sensitivity is linked to Lon protease deactivation

While POL CS in TIG-resistant *E. coli* has been previously reported [8,21], the mechanism of POL CS remains unknown. Since CS was abundant in strains evolved through all three platforms, we hypothesized that mutation(s) that 1) occurred in all three platforms, 2) appeared frequently and 3) appeared more frequently in strains exhibiting CS may be responsible for POL CS. We tallied the frequencies of each mutation stratified by CS and neutrality (Fig. 2B) (Supplementary Fig. 2) and found that the *lon*:IS186 mutation, previously reported to be a mutation hotspot [31], was the only mutation that met these criteria (Fig. 2B) (Supplementary Fig. 2).

Cells that lack Lon activity accumulate the transcriptional regular RcsA, which is a positive regulator of capsular polysaccharide (exopolysaccharide) synthesis [32,33]. Increased exopolysaccharides has been shown to increase sensitivity to POL by increasing concentration of POL around the outer membrane in *Klebsiella* [34]. We hypothesized that our TIG-resistant Lon mutants were overproducing exopolysaccharides, which in turn were making them more susceptible to POL. To test this, we randomly picked and grew three strains with the Lon mutation, three without the Lon mutation, and one with both the Lon and marR mutations on plates containing toluidine blue-O, congo red and ruthenium red. Toluidine blue-O binds to negatively charged polysaccharides, congo red binds to amyloid fibers like curli, and ruthenium red binds to acidic exopolysaccharides [35]. The Lon mutants were preferentially stained by toluidine blue-O and congo red (Fig. 2C), confirming that our Lon mutants overproduced exopolysaccharides. We did not see any difference between colonies grown on ruthenium red (data not shown). Based on these results, we propose that *lon*:IS186 mutants overproduce negatively charged exopolysaccharides which increase POL accumulation around the cells, rendering them hypersensitive towards the antibiotic (Fig. 2D).

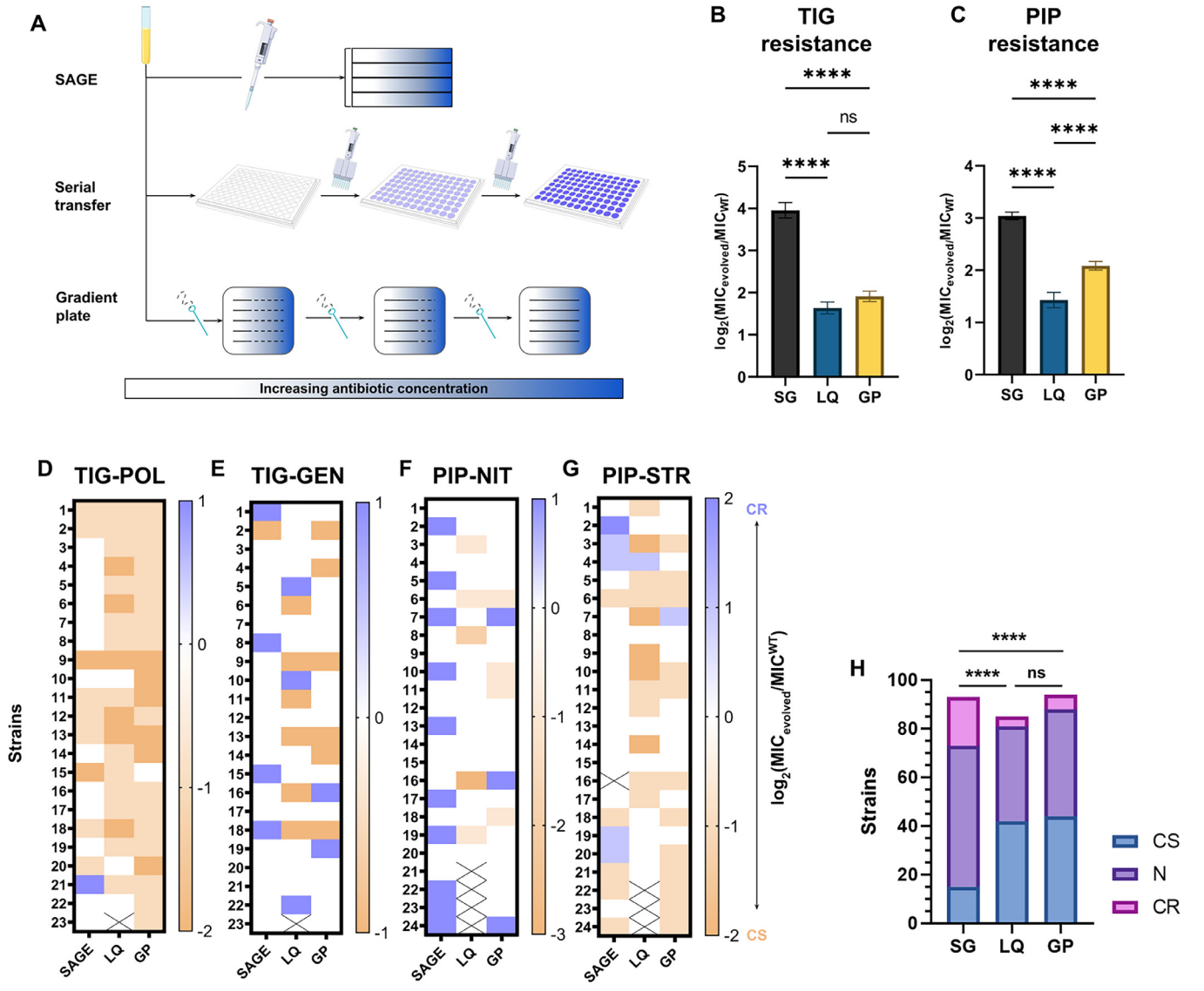

Fig. 1. Evolution of antibiotic resistance using three different ALEs. (A) Schematic of the ALE platforms used to evolve resistance in this study. SG = SAGE. (B) Relative TIG and (C) PIP MICs of evolved mutants. $^{****}P < 0.0001$, one-way ANOVA with Bonferroni correction. (D) - (G) CS profiles of mutants evolved to TIG and PIP. The labels on top show the antibiotics against which resistance was evolved and CS were measured. For example, "TIG-POL" denotes the POL CS measurements of TIG resistant mutants. (H) Combined CS, N and CR distributions from the three ALE platforms. SG = SAGE. $^{****}P < 0.0001$, one-way ANOVA with Bonferroni correction. Statistical analyses were performed by comparing relative MICs of mutants from each platform.

2.4. MarR deactivation neutralizes Lon deactivation-driven polymyxin collateral sensitivity

If Lon mutations produced the POL CS phenotype in the TIG-resistant cells, resistance to TIG that did not confer POL CS must have either occurred via a different pathway, or the CS effect of the Lon mutation may have been masked via secondary mutations. Candidate mutations that occurred frequently and preferentially in cells that remained neutral to POL were in the efflux regulators *acrR* and *marR* (Fig. 2B) (Supplementary Fig. 2), known to confer resistance to TIG [36,37]. This suggests that cells that bypass Lon mutations to achieve resistance via efflux upregulation avoid POL CS.

Fifty-five percent of the neutral strains also exhibited the Lon mutation (Fig. 2B). How do strains that carry this mutation mask the CS phenotype? To answer this question, we narrowed our analysis to the SAGE mutants, where we had an equal distribution of cells with CS and neutral phenotype sequenced (Supplementary Fig. 2). While 100% of the neutral strains had a MarR mutation, 67% of them also carried the *lon*:IS186 mutation. Since deactivation of MarR allows upregulation of TIG and POL efflux [29,30,38], we hypothesized that deactivation of MarR on a *lon*:IS186 background neutralizes the CS phenotype associated with Lon mutants (Fig. 2D). To test this, we constructed a pUC57-marR plasmid and introduced it into four POL-neutral strains that showed both the marR and *lon*:IS186 mutations. Strain 3 showed a 2 bp deletion mutation and strain 5 introduced a premature stop codon in marR (Table 1) which should both significantly reduce or completely abolish marR activity [39]. Mutation in the 104th amino acid that changes the glycine carried by strain 4 (Table 1) has been associated with reduced marR activity [40]. The AAGGCTGG duplication causes a frameshift mutation which should also affect marR activity (Table 1) [41]. Introduction of pUC67-marR converted three of the four strains from neutral to CS to POL, and increased susceptibility in the wildtype strain (Table 1). This suggested that cells that mutated MarR gained the ability to resist POL at a magnitude large

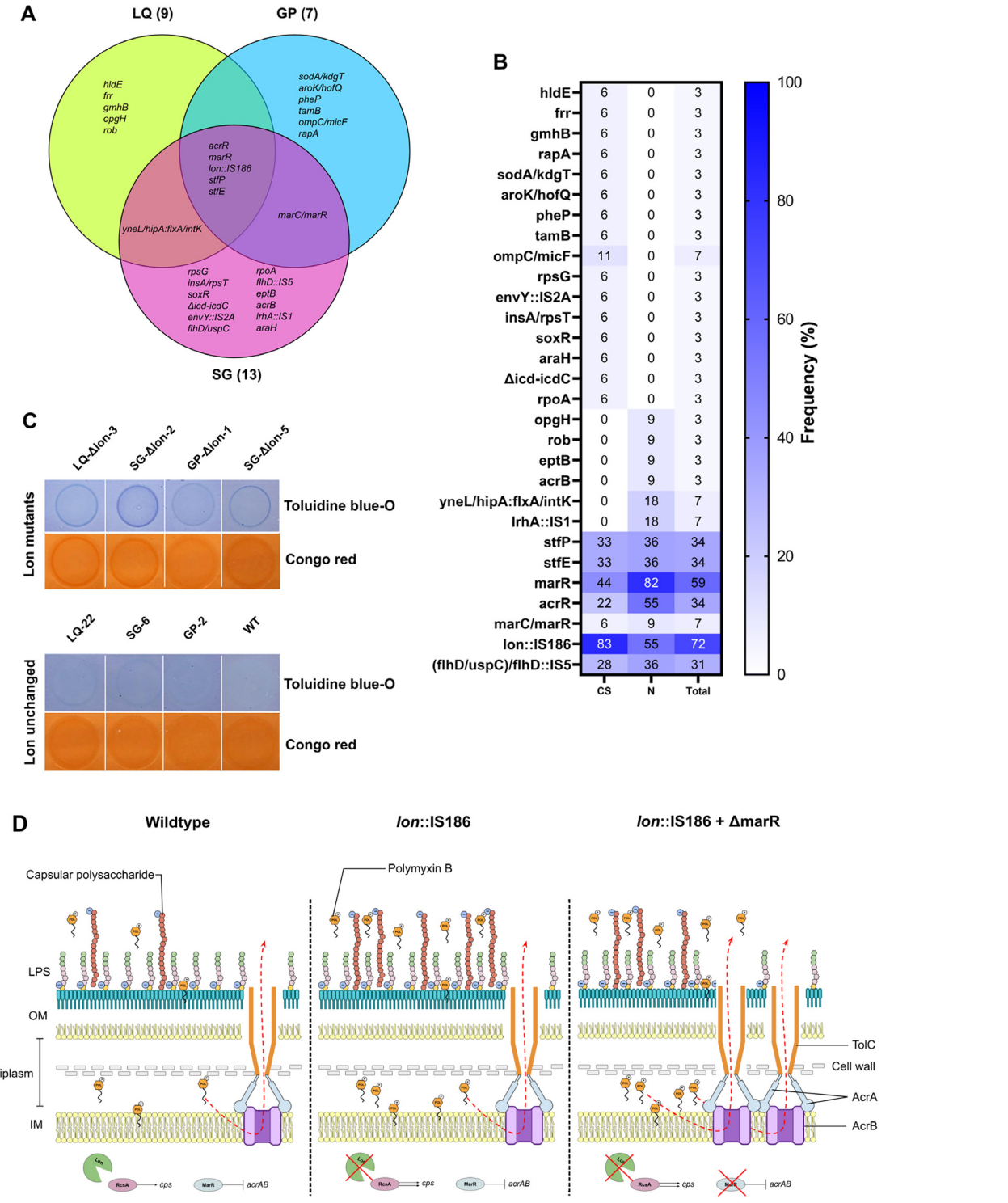

Fig. 2. Genomic and phenotypic analysis reveals mechanism of POL CS in TIG resistant mutants. (A) Venn diagram showing common mutations between TIG mutants evolved from the three different platforms. The numbers in brackets denote the total number of mutants sequenced from that platform. (B) Frequency at which a mutation in the genes listed on the vertical axis appeared in all 29 mutants sequenced in this study, stratified by POL CS and N. "Total" denotes frequencies at which a mutation appeared among all strains. "sodA/kdgT" refers to an intergenic mutation between the genes *sodA* and *kdgT*. "envY:IS2A" denotes that gene *envY* was interrupted by the insertion element IS2A. "Δicd-icdC" refers to a deletion that affects all genes between and including *icd* and *icdC*. "yneL/hipA:flxA/intK" refers to a new junction between the intergenic regions of *yneL/hipA* and *flxA/intK*. Two different *flhD* mutations: (flhD/uspC) and flhD:IS5 were grouped together and reported as "(flhD/uspC)/flhD:IS5". (C) Toluidine blue-O and Congo red binding assays for four randomly picked Lon mutants and four with Lon intact. The strain IDs of the mutants are noted at the top of the panels. Strain IDs contain information about the platform used, and the lineage that was picked. For example, "LQ-Δlon-3" = Lon mutant from the LQ platform, with "3" denoting that it is the third lineage out of the 22 generated through this platform. "LQ-22" = the 22nd lineage from the platform, with no mutation in Lon. WT = wildtype. (D) The role of Lon and MarR mutations in POL CS. Left panel: WT cells. Lon degrades RcsA, limiting the expression of capsular polysaccharide genes (cps). MarR expression negatively regulates *acrAB* expression. Middle panel: Lon deactivation to evolve TIG resistance spares RcsA from degradation, allowing expression of cps genes and causing the production of capsular polysaccharides. Increased negative charge on the membrane due to these polysaccharides causes increased accumulation of the polycationic POL, making cells more susceptible to POL. Right panel: MarR-deactivating mutations associated with TIG resistance allow increased *acrAB* expression, increasing the number of efflux pumps that are able to pump out POL molecules, neutralizing POL CS.

Table 1
Changes in POL MIC after introduction of the pUC57-marR plasmid in strains with different MarR mutations.

Strain	MarR allele	POL MIC (μg/mL)
WT	-	0.25
TIG-SG-N-3	Δ2 bp coding (428–429/435 nt)	0.25
TIG-SG-N-4	G104S	0.25
TIG-SG-N-5	Q117*	0.25
TIG-SG-N-7	$(AAGGCTGG)_{1\rightarrow2}$	0.25
WT + pUC57	-	0.25
TIG-SG-N-3 + pUC57	Δ2 bp coding (428–429/435 nt)	0.25
TIG-SG-N-4 + pUC57	G104S	0.25
TIG-SG-N-5 + pUC57	Q117*	0.25
TIG-SG-N-7 + pUC57	$(AAGGCTGG)_{1\rightarrow2}$	0.125
WT + pUC57-marR	-	0.125
TIG-SG-N-3 + pUC57-marR	Δ2 bp coding (428–429/435 nt)	0.125
TIG-SG-N-4 + pUC57-marR	G104S	0.125
TIG-SG-N-5 + pUC57-marR	Q117*	0.125
TIG-SG-N-7 + pUC57-marR	$(AAGGCTGG)_{1\rightarrow2}$	0.125

enough to neutralize CS due to the *lon*:IS186 mutation. Reintroduction of MarR on a plasmid then reduced efflux levels, reverting the effects of the MarR mutation.

MarR mutations cannot completely explain neutrality: a significant number of strains that carried *marR* mutations showed CS towards POL (Fig. 2B) (Supplementary Fig. 2). Additional mutations in these strains such as HldE (D-beta-D-heptose 7-phosphate kinase), GmhB (D–glycero-beta-D-manno-heptose-1,7-bisphosphate 7-phosphatase) and TamB (translocation and assembly module subunit) (Fig. 2B) (Supplementary Fig. 2) involved in LPS biosynthesis and maintenance [29,42,43] and may have played a role in POL sensitivity.

2.5. Strong intra-class cross-resistance, but not collateral sensitivity, is prevalent in clinical E. coli

The goal of identifying any CS relationship is to ultimately apply it in antibiotic sequences or combinations that are resilient against resistance evolution in the clinic. To test for the presence of collateral effects of resistance in pathogenic *E. coli*, we calculated the Pearson correlation coefficients between MIC data to serve as a proxy for cross resistances and collateral sensitivities from 779 uropathogenic *E. coli* strains from the CANWARD surveillance study (Supplementary Table 2) [37]. We identified strong cross-resistance between drugs of the same class, particularly between β-lactams (Fig. 3A). Very little negative correlation was present in the dataset, which appears to be common in clinical datasets [44]. The largest negative correlation of −0.05 was seen between omadacycline (OMC) and colistin (COL).

2.6. CS relationships rarely appear in clinical strains and their prevalence is best predicted by SAGE

We looked more closely at the clinical antibiotic susceptibility data to identify smaller changes in resistance. Specifically, we looked at the TIG-GEN, PIP-NIT and TIG-POL relationships to compare with our ALE results. PIP-STR was not included since STR was not among the drugs in the clinical dataset. Since our ALE adaptations only included chromosomal changes, it was important to limit our analysis to resistance conferred by chromosomal mutations instead of mobile elements. TIG is unaffected by *tet(M)*, *tet(A)*, *tet(B)*, *tet(C)*, *tet(D)*, and *tet(K)* mobile resistance determinants [45]. Plasmid-encoded *tet(X)* genes that code for TIG-inactivating enzymes and confer high TIG resistance with MICs ranging from 8 to 16 μg/mL are rare [46,47], and our dataset did not contain TIG MICs >2 μg/mL. Chromosomal TIG resistance generally arises from increased efflux mediated by AcrAB-TolC in *E. coli* [30], and to further confirm that TIG resistance was largely chromosome mediated in our clinical dataset, we hypothesized that PIT (piperacillin/tazobactam) resistance should go up with increasing TIG resistance since PIP is susceptible to efflux. As expected, PIT resistance did increase with increasing TIG MIC in the clinical strains (Fig. 3B).

Next, we looked at how GEN MICs varied with increasing TIG MIC. We removed GEN MICs > 4 μg/mL from the analysis because these MICs were more likely to be conferred by plasmid-borne aminoglycoside modifying enzymes [48]. We observed a steady increase in GEN MICs with increasing TIG MIC among the remaining isolates (Fig. 3C). From our ALE experiments, LQ and GP showed CS in over 25% of the strains, but SAGE in ∼4%, while CR was present in 17% of strains (Fig. 1E) (Supplementary Fig. 1).

NIT MIC changes with PIT resistance did not reach statistical significance, but showed an increasing trend up to 8 μg/mL of PIT resistance. From the ALE results, LQ and GP lineages showed CS in 17-25% of the strains with none from SAGE (Fig. 1F) (Supplementary Fig. 1). Over 40% of the SAGE lineages were cross-resistant to NIT (Fig. 1F) (Supplementary Fig. 1).

POL was not included in the clinical antimicrobial susceptibility data, so we examined the TIG-colistin (COL) relationship instead. Colistin and POL have very similar structures and near-identical activity *in vitro* [49]. For the first time in the analysis, we see small but statistically insignificant reductions in COL resistance with up to 0.5 μg/mL of TIG MIC (Fig. 3E). During this analysis, we observed that mean COL resistance dropped significantly with resistance to another third generation tetracycline, omadacycline (OMC) (Fig. 3F, G) [50]. As OMC MIC increased from 0.5 to 1 μg/mL, COL MIC dropped ∼three-fold (Fig. 3F). ∼86-96% of LQ and GP lineages and ∼39% of SAGE lineages showed CS to POL (Fig. 1D) (Supplementary Fig. 1).

3. Discussion

In this study we investigated the repeatability of CS evolution in four reported drug pairs. With large sample sizes of 20-24 lineages we examined three different ALE platforms, testing the robustness of CS interactions to changes in evolutionary conditions and identifying possible ALE-specific biases. We found that SAGE allowed rapid evolution of high level resistance to antibiotics while still producing core resistance-conferring mutations comparable to other ALE platforms (Fig. 1B, C) (Fig. 2A) (Supplementary Fig. 2). SAGE consistently produced lower frequencies of CS and higher cases of CR compared to the serial transfer and gradient plating-based methods (Fig. 1D–G) in the TIG - GEN, PIP - NIT and PIP - STR drug pairs. This best matched antimicrobial susceptibility data from over 750 clinical MDR *E. coli* strains, in which CR and neutrality were abundant but indications of CS relationships were almost entirely absent (Fig. 3A). Importantly, we found no negative correlations between TIG - GEN, PIP - NIT and PIP –STR resistances, and instead found evidence of cross-resistance (Fig. 3C–E). This suggests that while CS relationships may regularly appear through laboratory evolutions, their application in the clinic needs to be carefully assessed. If the effect of CS is minimal in clinical strains, the usefulness of CS relationships elucidated from ALE experiments may be inflated. Out of the four drug pairs tested, SAGE produced substantial CS in only one of them, the TIG - POL pair (∼39%; Fig. 1D, H). From the clinical data, we observed that resistance to COL decreased with another third-generation tetracycline, omadacyline (Fig. 3F) [50]. The fact that this CS relationship appeared frequently in all three ALE platforms (Fig. 1D) and held among MDR clinical strains suggests that this could be potentially exploitable to select against resistance, and that SAGE may be able to predict these important relationships.

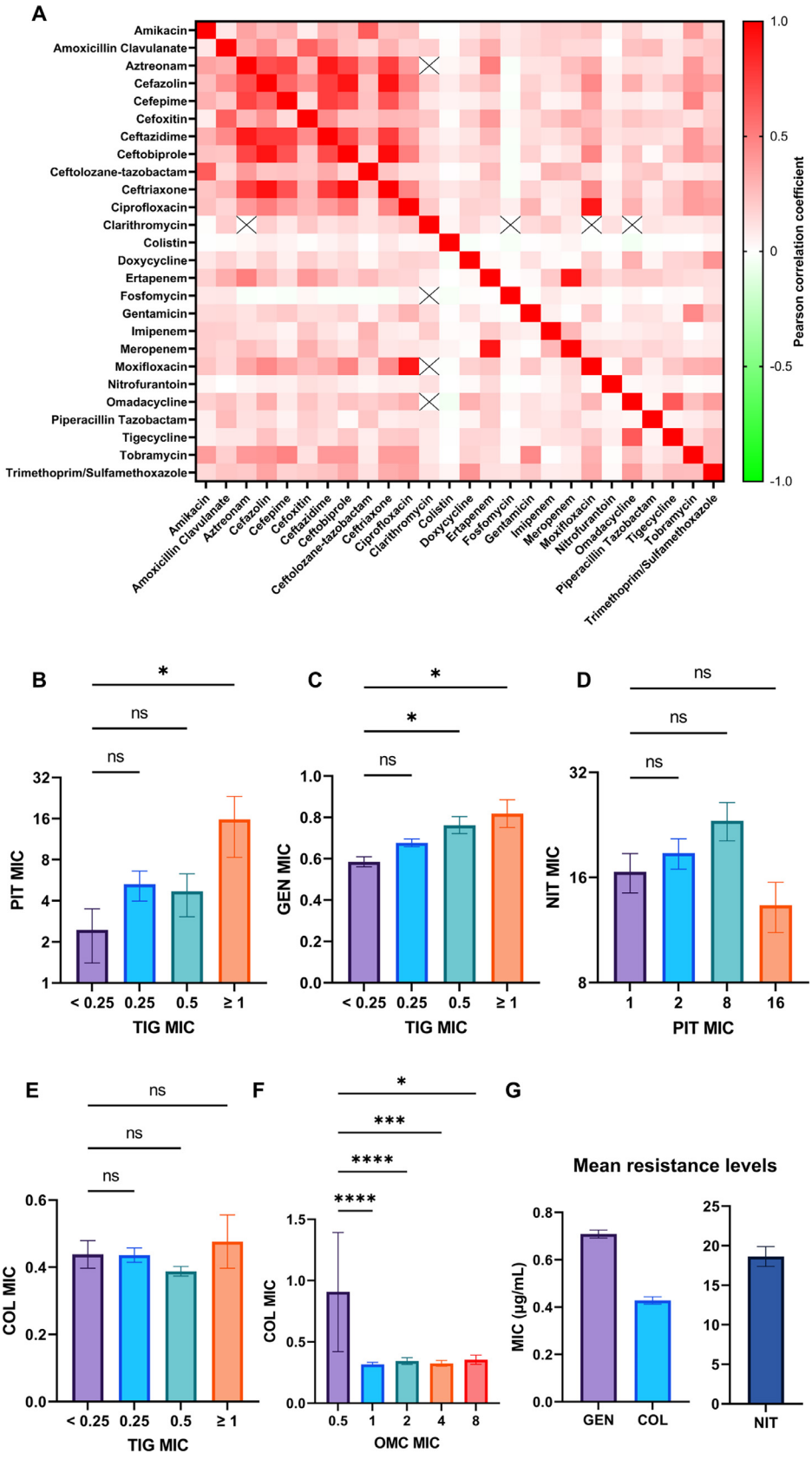

Fig. 3. Uropathogenic *E. coli* antimicrobial susceptibilities reveals a rare CS relationship predicted by laboratory evolution. (A) Pearson correlation coefficients between MICs of each antibiotic with every other antibiotic in the dataset. A value of 1 denotes a perfect positive correlation (strong CR), 0 denotes no correlation, while a −1 denotes a perfect negative correlation (strong CS). (B) - (F) Relationship between resistances to drugs labelled on the x- and y-axes. $^{*}P < 0.05$, $^{***}P < 0.001$, $^{****}P < 0.0001$, one-way ANOVA with Bonferroni correction. (G) Mean resistance levels of antibiotics on the x-axis from the whole dataset.

We previously showed the presence of reciprocal CS between the TIG-POL drug pair [21], but the mechanism of CS was unknown. In this study we showed that tigecycline-resistant Lon mutants produced increased extracellular polysaccharides, rendering them more susceptible to POL. From the ubiquity of the Lon mutations in our data and prior reports, it is likely that this mutation is the first step towards clinical TIG resistance [30,51], and hence the COL sensitivity in clinical strains may be driven by the same mechanism. Cells may bypass the CS to POL by either increasing efflux through mutations in regulators like MarR, or by acquiring second step efflux regulator mutations after Lon deactivation (Fig. 2B–D), suggesting the observed COL sensitivity may be transitory or that increased efflux may have undetected fitness costs.

Second step mutations in efflux regulators AcrR and MarR appeared more frequently in SAGE compared to LQ and GP (Supplementary Fig. 2) and could partly be responsible for the low CS in SAGE lineages. In contrast to our findings, one study showed that accumulation of second step resistance mutations conferred collateral sensitivity over resistance to antibiotics [52]. However, in that study, efflux mutations were the first step mutations, with second step mutations conferring the CS they observed [52]. This is in line with our and others' findings that efflux mutations often confer broad-spectrum CR [53,54]. Another study showed how CS varies at a population level, with lineages that showed CS early during evolution getting replaced by mutants that acquired changes in genes with milder CS effects [11]. Our results suggest that this can also occur at the strain level. Together, we suggest that the evolutionary timeline of CS cannot be generalized and must be studied on a case-by-case basis, possibly at the antibiotic and the bacterial species level.

The usefulness of CS has been debated, due in part to its dependence on the repeatability of evolution [55]. Our results show that CS can indeed often appear at only low frequencies (Fig. 1E–G), and is strongly linked to the specific mechanism by which cells become resistant. Our highly repeatable TIG-POL CS relationship was dependent on selection of the same *lon*:IS186 mutation across almost all sequenced lineages that exhibited CS. While this limits the number of CS interactions that may be worth pursuing, this also offers hope that robust CS that appear in complicated evolutionary landscapes in healthcare may be achieved via targeting collateral effects tied to readily accessible mutational hotspots.

From our attempts at evolving large sample sizes against multiple antibiotics via the different ALEs, we found that generating large numbers of resistant mutants was easier with SAGE (Supplementary Table 1), though the number of mutations per strain and the core resistance determinants selected for were similar to the other platforms tested (Fig. 2A). This should facilitate ALE experimentation at scale in laboratories that do not have ready access to robotics.

Overall, we discovered a mechanism by which TIG resistance reliably conferred CS to POL by leveraging large scale laboratory evolution and showed that these biological effects were observed and reproducible in more than 750 clinical MDR *E. coli* strains. We highlighted the importance of large scale ALE experiments to generate robust profiles of collateral effects and showed that SAGE better predicts CS relationships that can help reduce antibiotic resistance in the clinic.

4. Materials and Methods

4.1. Bacterial strain and growth conditions

E. coli K-12 substr. BW25113 (WT) was grown aerobically at 37°C with 250 rpm shaking in cation-adjusted Muller Hinton (MH) broth. All evolved mutants were grown in MH broth supplemented with appropriate concentration of antibiotics.

4.1.1. Susceptibility assays

MICs were performed using the EUCAST standard broth microdilution method [56].

4.1.2. ALE experiments

SAGE, serial transfer and gradient plating-based evolutions were performed as described before [18–21,53,57]. To prepare a SAGE plate, MH media with 0.15% agar was stirred and heated, followed by slow addition of 0.2% xanthan gum before autoclaving [20]. This liquid was supplemented with antibiotics and poured into 4-well plates that were propped up on one side using p1000 pipette tips. After this layer was set, a second layer of antibiotic free medium was added to create an even surface, and plates were incubated overnight at room temperature to allow diffusion. For SAGE, the maximum concentration of antibiotics are listed in the table below. Maximum concentrations were determined from experiments to determine suitable concentrations that consistently generated mutants above clinical breakpoints. All SAGE plates were incubated for a fixed duration of seven days, which we found to be sufficient for cells to reach the end of the plates [21,58]. For serial transfers, evolutions were started at $1/8^{th}$ the WT MIC of the antibiotic by transferring 1 uL of overnight culture of WT bacteria into 99 uL of MH broth containing appropriate concentration of the antibiotic. Plates were incubated for 18-20 h, then 1 uL from all wells showing growth were transferred onto the $1/4^{th}$ MIC plate and so on, until the concentration listed in the table below was reached (i.e., a total of six transfers). Passaging beyond the listed concentration incurred significant loss of strains due to extinctions. For gradient plates, maximum antibiotic concentrations are listed below. Plates were made in square dishes (Falcon, Cat. No.: 351112) and were streaked towards the higher end of the antibiotic gradient after 18–20 h of incubation until growth was observed within the last grid of the plates.

Antibiotic	Maximum concentration in SAGE
TIG	5 μg/mL
PIP	40 μg/mL

Antibiotic	Maximum concentration evolved to during serial transfers
TIG	4x MIC, 1 μg/mL
PIP	4x MIC, 4 μg/mL

Antibiotic	Maximum concentration in gradient plates	Days taken to reach end of plates
TIG	5 μg/mL	5 days
PIP	80 μg/mL	5-7 days

4.1.3. Whole genome sequencing and analysis

Genomes were extracted using the Bio Basic genomic DNA kit (Cat. no.: BS624). Sequencing and variant calling was performed by Seqcenter (USA), on an Illumina NextSeq 2000. Variant calling was carried out using Breseq (80). Reference sequence CP009273.1 was used for variant calling. All mutations reported had a frequency of a 100% over a sequencing depth of ~100–120x. Coverage of 99–100% was achieved for all mutants sequenced. WGS data is available under the NCBI Sequence Read Archive BioProject: PRJNA1220725NCBI. Fig. 2 and Supplementary Fig. 2 were built using R and GraphPad Prism.

4.1.4. Exopolysaccharide assay

MH + 1.5% agar was separately supplemented with 150 µg/ml Congo red, 40 µg/ml toluidine blue O or 40 µg/ml ruthenium red (AK Scientific) [35]. All plates also contained 0.5 μg/mL of TIG. 10

uL of overnight cultures grown in MH broth + 0.5 μg/mL of TIG were spotted onto these plates.

4.1.5. MarR complementation

The *marR* fragment was synthesized based on its sequence available in the NCBI reference sequence CP009273.1, and inserted into the pUC57 MCS by Bio Basic Inc. The ligated plasmid was sequence verified before use in experiments. Cells were chemically transformed separately with the empty vector or pUC57-marR [59]. We determined from separate experiments with this plasmid that IPTG induction was not required for sufficient marR production: cells transformed with this plasmid showed reduced efflux activity as measured by chloramphenicol resistance [60] but increasing concentrations of IPTG did not significantly change this resistance level (data not shown).

4.1.6. Clinical strains and data analysis

Antibiotic susceptibility data of 779 uropathogenic *E. coli* strains was obtained from the CANWARD surveillance study [61]. The Pearson correlation coefficients and MIC data extraction were performed using custom Python scripts.

Data and materials availability

WGS data is available under the NCBI Sequence Read Archive BioProject: PRJNA1220725. All other relevant data is included in the main text and supplementary material. Strains are available upon request.

Ethical approval

Not required.

Declaration of competing interest

The authors declare no competing interest.

Funding

This study was funded by the Fonds de recherche du Québec – Santé (FRQS) (269182). FRC is supported by the Fonds de recherche du Québec –Santé (FRQS) (B2X). Veronica Banari was funded by DAAD Rise Worldwide during a Mitacs Globalink Research Internship. We thank L. Freeman for helpful discussions.

Supplementary materials

Supplementary material associated with this article can be found, in the online version, at doi:10.1016/j.ijantimicag.2025.107564.

References

[1] Naghavi M, Vollset SE, Ikuta KS, Swetschinski LR, Gray AP, Wool EE, et al. Global burden of bacterial antimicrobial resistance 1990-2021: a systematic analysis with forecasts to 2050. Lancet 2024;404:1199–226. doi:10.1016/S0140-6736(24)01867-1.

[2] Bo L, Sun H, Li Y-D, Zhu J, Wurpel JND, Lin H, et al. Combating antimicrobial resistance: the silent war. Front Pharmacol 2024;15. doi:10.3389/fphar.2024.1347750.

[3] Roemhild R, Barbosa C, Beardmore RE, Jansen G, Schulenburg H. Temporal variation in antibiotic environments slows down resistance evolution in pathogenic Pseudomonas aeruginosa. Evol Appl 2015;8:945–55. doi:10.1111/eva.12330.

[4] Merker M, Tueffers L, Vallier M, Groth EE, Sonnenkalb L, Unterweger D, et al. Evolutionary approaches to combat antibiotic resistance: opportunities and challenges for precision medicine. Front Immunol 2020;11.

[5] Imamovic L, Ellabaan MMH, Machado AMD, Citterio L, Wulff T, Molin S, et al. Drug-driven phenotypic convergence supports rational treatment strategies of chronic infections. Cell 2018;172:121 -134.e14. doi:10.1016/j.cell.2017.12.012.

[6] Barbosa C, Römhild R, Rosenstiel P, Schulenburg H. Evolutionary stability of collateral sensitivity to antibiotics in the model pathogen Pseudomonas aeruginosa. eLife 2019;8:e51481. doi:10.7554/eLife.51481.

[7] Roemhild R, Andersson DI. Mechanisms and therapeutic potential of collateral sensitivity to antibiotics. PLOS Pathog 2021;17:e1009172. doi:10.1371/JOURNAL.PPAT.1009172.

[8] Imamovic L, Sommer MOA. Use of collateral sensitivity networks to design drug cycling protocols that avoid resistance development. Sci Transl Med 2013;5:204ra132 -204ra132. doi:10.1126/SCITRANSLMED.3006609.

[9] Podnecky NL, Fredheim EGA, Kloos J, Sørum V, Primicerio R, Roberts AP, et al. Conserved collateral antibiotic susceptibility networks in diverse clinical strains of Escherichia coli. Nat Commun 2018;9:3673. doi:10.1038/s41467-018-06143-y.

[10] Hernando-Amado S., Sanz-García F., Martínez J. Rapid and robust evolution of collateral sensitivity in Pseudomonas aeruginosa antibiotic-resistant mutants 2020. https://doi.org/10.1126/sciadv.aba5493.

[11] Sakenova N, Cacace E, Orakov A, Huber F, Varik V, Kritikos G, et al. Systematic mapping of antibiotic cross-resistance and collateral sensitivity with chemical genetics. Nat Microbiol 2024:1–15. doi:10.1038/s41564-024-01857-w.

[12] Allen RC, Pfrunder-Cardozo KR, Hall AR. Collateral sensitivity interactions between antibiotics depend on local abiotic conditions. mSystems 2021;6:e01055 -21. doi:10.1128/mSystems.01055-21.

[13] Hernando-Amado S, Laborda P, Martínez JL. Tackling antibiotic resistance by inducing transient and robust collateral sensitivity. Nat Commun 2023;14:1723. doi:10.1038/s41467-023-37357-4.

[14] Jahn LJ, Munck C, Ellabaan MMH, Sommer MOA. Adaptive laboratory evolution of antibiotic resistance using different selection regimes lead to similar phenotypes and genotypes. Front Microbiol 2017;8. doi:10.3389/fmicb.2017.00816.

[15] Laborda P, Martínez JL, Hernando-Amado S. Evolution of habitat-dependent antibiotic resistance in Pseudomonas aeruginosa. Microbiol Spectr 2022;10:e00247 -22. doi:10.1128/spectrum.00247-22.

[16] Krajewska J, Tyski S, Laudy AE. In vitro resistance-predicting studies and In vitro resistance-related parameters—A hit-to-lead perspective. Pharmaceuticals 2024;17:1068. doi:10.3390/ph17081068.

[17] Ghaddar N., Hashemidahaj M., Findlay B.L. Access to high-impact mutations constrains the evolution of antibiotic resistance in soft agar. Sci Rep 2018;8:1-10. https://doi.org/10.1038/s41598-018-34911-9.

[18] Vinchhi R, Jena C, Matange N. Adaptive laboratory evolution of antimicrobial resistance in bacteria for genetic and phenotypic analyses. STAR Protoc 2023;4:102005. doi:10.1016/j.xpro.2022.102005.

[19] Szybalski W, Bryson V. Genetic studies on microbial cross resistance to toxic agents i. J Bacteriol 1952;64:489–99. doi:10.1128/jb.64.4.489-499.1952.

[20] Chowdhury FR, Mercado LD, Kharitonov K, Findlay BL. De novo evolution of antibiotic resistance to Oct-TriA1. Microbiol Res 2025;293:128056. doi:10.1016/j.micres.2025.128056.

[21] Chowdhury F.R., Findlay B.L. Backward collateral sensitivity can restore antibiotic susceptibility. https://doi.org/10.1101/2024.11.06.622341.

[22] Culp EJ, Waglechner N, Wang W, Fiebig-Comyn AA, Hsu Y-P, Koteva K, et al. Evolution-guided discovery of antibiotics that inhibit peptidoglycan remodelling. Nature 2020;578:582–7. doi:10.1038/s41586-020-1990-9.

[23] Goig GA, Menardo F, Salaam-Dreyer Z, Dippenaar A, Streicher EM, Daniels J, et al. Effect of compensatory evolution in the emergence and transmission of rifampicin-resistant mycobacterium tuberculosis in Cape Town, South Africa: a genomic epidemiology study. Lancet Microbe 2023;4:e506 -15. doi:10.1016/S2666-5247(23)00110-6.

[24] Eckartt KA, Delbeau M, Munsamy-Govender V, DeJesus MA, Azadian ZA, Reddy AK, et al. Compensatory evolution in NusG improves fitness of drug-resistant M. tuberculosis. Nature 2024;628:186–94. doi:10.1038/s41586-024-07206-5.

[25] Loftie-Eaton W, Bashford K, Quinn H, Dong K, Millstein J, Hunter S, et al. Compensatory mutations improve general permissiveness to antibiotic resistance plasmids. Nat Ecol Evol 2017;1:1354–63. doi:10.1038/s41559-017-0243-2.

[26] Szamecz B, Boross G, Kalapis D, Kovács K, Fekete G, Farkas Z, et al. The genomic landscape of compensatory evolution. PLOS Biol 2014;12:e1001935. doi:10.1371/journal.pbio.1001935.

[27] Li F, Wang J, Jiang Y, Guo Y, Liu N, Xiao S, et al. Adaptive evolution compensated for the plasmid fitness costs brought by specific genetic conflicts. Pathogens 2023;12:137. doi:10.3390/pathogens12010137.

[28] Olivares Pacheco J, Alvarez-Ortega C, Alcalde Rico M, Martínez JL. Metabolic compensation of fitness costs is a general outcome for antibiotic-resistant Pseudomonas aeruginosa mutants overexpressing efflux pumps. mBio 2017;8:e00500 -17. doi:10.1128/mBio.00500-17.

[29] Linkevicius M, Sandegren L, Andersson DI. Mechanisms and fitness costs of tigecycline resistance in Escherichia coli. J Antimicrob Chemother 2013;68:2809–19. doi:10.1093/jac/dkt263.

[30] Grossman TH. Tetracycline antibiotics and resistance. Cold Spring Harb Perspect Med 2016;6:a025387. doi:10.1101/cshperspect.a025387.

[31] SaiSree L, Reddy M, Gowrishankar J. IS186 Insertion at a hot spot in thelon promoter as a basis for Lon protease deficiency ofEscherichia coli B: identification of a consensus target sequence for IS186 transposition. J Bacteriol 2001;183:6943–6. doi:10.1128/jb.183.23.6943-6946.2001.

[32] Stout V, Torres-Cabassa A, Maurizi MR, Gutnick D, RcsA Gottesman S. an unstable positive regulator of capsular polysaccharide synthesis. J Bacteriol 1991;173:1738–47. doi:10.1128/jb.173.5.1738-1747.1991.

[33] Torres-Cabassa AS, Gottesman S. Capsule synthesis in Escherichia coli K-12 is regulated by proteolysis. J Bacteriol 1987;169:981–9. doi:10.1128/jb.169.3.981-989.1987.
[34] D'Angelo F., Rocha E.P.C., Rendueles O. The capsule increases susceptibility to last-resort polymyxins, but not to other antibiotics, in Klebsiella pneumoniae. Antimicrob Agents Chemothe;67:e00127-23. https://doi.org/10.1128/aac.00127-23.
[35] Lionel Ferrières, Aslam SN, Cooper RM, Clarke DJ. The yjbEFGH locus in Escherichia coli K-12 is an operon encoding proteins involved in exopolysaccharide production. Microbiology 2007;153:1070–80. doi:10.1099/mic.0.2006/002907-0.
[36] Ma X, Xi W, Yang D, Zhao L, Yu W, He Y, et al. Collateral sensitivity between tetracyclines and aminoglycosides constrains resistance evolution in carbapenem-resistant Klebsiella pneumoniae. Drug Resist Updat 2023;68:100961. doi:10.1016/j.drup.2023.100961.
[37] Sharma P, Haycocks JRJ, Middlemiss AD, Kettles RA, Sellars LE, Ricci V, et al. The multiple antibiotic resistance operon of enteric bacteria controls DNA repair and outer membrane integrity. Nat Commun 2017;8:1444. doi:10.1038/s41467-017-01405-7.
[38] Warner DM, Levy SB. Different effects of transcriptional regulators MarA, SoxS and Rob on susceptibility of Escherichia coli to cationic antimicrobial peptides (CAMPs): rob-dependent CAMP induction of the marRAB operon. Microbiology 2010;156:570–8. doi:10.1099/mic.0.033415-0.
[39] Williams LE, Wernegreen JJ. Sequence context of indel mutations and their effect on protein evolution in a bacterial endosymbiont. Genome Biol Evol 2013;5:599–605. doi:10.1093/gbe/evt033.
[40] Kumaraswami M, Schuman JT, Seo SM, Kaatz GW, Brennan RG. Structural and biochemical characterization of MepR, a multidrug binding transcription regulator of the Staphylococcus aureus multidrug efflux pump MepA. Nucleic Acids Res 2009;37:1211–24. doi:10.1093/nar/gkn1046.
[41] Huseby DL, Brandis G, Hughes D. Fitness cost constrains the spectrum of marR mutations in ciprofloxacin-resistant Escherichia coli. J Antimicrob Chemother 2017;72:3016–24. doi:10.1093/jac/dkx270.
[42] Kneidinger B, Marolda C, Graninger M, Zamyatina A, McArthur F, Kosma P, et al. Biosynthesis pathway of ADP-L-glycero-β-D-manno-heptose in Escherichia coli. J Bacteriol 2002;184:363–9. doi:10.1128/jb.184.2.363-369.2002.
[43] Josts I, Stubenrauch CJ, Vadlamani G, Mosbahi K, Walker D, Lithgow T, et al. The structure of a conserved domain of TamB reveals a hydrophobic β taco fold. Structure 2017;25:1898 -1906.e5. doi:10.1016/j.str.2017.10.002.
[44] Herencias C, Álvaro-Llorente L, Ramiro-Martínez P, Fernández-Calvet A, Muñoz-Cazalla A, DelaFuente J, et al. β-lactamase expression induces collateral sensitivity in Escherichia coli. Nat Commun 2024;15:4731. doi:10.1038/s41467-024-49122-2.
[45] Petersen PJ, Jacobus NV, Weiss WJ, Sum PE, In Testa RT. Vitro and In vivo antibacterial activities of a novel glycylcycline, the 9-t-butylglycylamido derivative of minocycline (GAR-936). Antimicrob Agents Chemother 1999;43:738–44. doi:10.1128/aac.43.4.738.
[46] Zeng Y, Lu J, Liu C, Ling Z, Sun Q, Wang H, et al. A method for screening tigecycline-resistant gene *tet*(X) from human gut. J Glob Antimicrob Resist 2021;24:29–31. doi:10.1016/j.jgar.2020.11.010.
[47] Sun J, Chen C, Cui C-Y, Zhang Y, Liu X, Cui Z-H, et al. Plasmid-encoded tet(X) genes that confer high-level tigecycline resistance in Escherichia coli. Nat Microbiol 2019;4:1457–64. doi:10.1038/s41564-019-0496-4.
[48] Jakobsen L, Sandvang D, Jensen VF, Seyfarth AM, Frimodt-Møller N, Hammerum AM. Gentamicin susceptibility in *Escherichia coli* related to the genetic background: problems with breakpoints. Clin Microbiol Infect 2007;13:830–2. doi:10.1111/j.1469-0691.2007.01751.x.
[49] Nation RL, Velkov T, Li J. Colistin and Polymyxin B: peas in a pod, or chalk and cheese? Clin Infect Dis Off Publ Infect Dis Soc Am 2014;59:88–94. doi:10.1093/cid/ciu213.
[50] Heidrich CG, Mitova S, Schedlbauer A, Connell SR, Fucini P, Steenbergen JN, et al. The novel aminomethylcycline omadacycline has high specificity for the primary tetracycline-binding site on the bacterial ribosome. Antibiotics 2016;5:32. doi:10.3390/antibiotics5040032.
[51] Nicoloff H, Andersson DI. Lon protease inactivation, or translocation of the gene, potentiate bacterial evolution to antibiotic resistance. Mol Microbiol 2013;90:1233–48. doi:10.1111/mmi.12429.
[52] Maltas J, Huynh A, Wood KB. Dynamic collateral sensitivity profiles highlight opportunities and challenges for optimizing antibiotic treatments. PLOS Biol 2025;23:e3002970. doi:10.1371/journal.pbio.3002970.
[53] Chowdhury FR, Findlay BL. Fitness costs of antibiotic resistance impede the evolution of resistance to other antibiotics. ACS Infect Dis 2023;9:1834–45. doi:10.1021/acsinfecdis.3c00156.
[54] Webber MA, Piddock LJV. The importance of efflux pumps in bacterial antibiotic resistance. J Antimicrob Chemother 2003;51:9–11. doi:10.1093/jac/dkg050.
[55] Nichol D., Rutter J., Bryant C., Hujer A.M., Lek S., Adams M.D., et al. Antibiotic collateral sensitivity is contingent on the repeatability of evolution. Nat Commun 20191012019;10:1-10. https://doi.org/10.1038/s41467-018-08098-6.
[56] EUCAST: MIC determination 2025 https://www.eucast.org/ast_of_bacteria/mic_determination/?no_cache=1 (accessed December 25, 2021).
[57] Krist AC, Showsh SA. Experimental evolution of antibiotic resistance in bacteria. Am Biol Teach 2007;69:94–7. doi:10.1662/0002-7685(2007)69[94:EEOARI]2.0.CO;2.
[58] Chowdhury F.R., Findlay B.L. Tripartite loops reverse antibiotic resistance 2025:2025.01.04.631305. https://doi.org/10.1101/2025.01.04.631305.
[59] Chung CT, Niemela SL, Miller RH. One-step preparation of competent Escherichia coli: transformation and storage of bacterial cells in the same solution. Proc Natl Acad Sci U S A 1989;86:2172–5. doi:10.1073/pnas.86.7.2172.
[60] Langevin AM, El Meouche I, Dunlop MJ. Mapping the role of AcrAB-TolC efflux pumps in the evolution of antibiotic resistance reveals near-MIC treatments facilitate resistance acquisition. mSphere 2020;5:e01056 -20. doi:10.1128/mSphere.01056-20.
[61] Denisuik AJ, Garbutt LA, Golden AR, Adam HJ, Baxter M, Nichol KA, et al. Antimicrobial-resistant pathogens in Canadian ICUs: results of the CANWARD 2007 to 2016 study. J Antimicrob Chemother 2019;74:645–53. doi:10.1093/jac/dky477.